Observer Performance of Reduced X-Ray Images on Liquid Crystal Displays

Akiko Ihori[1*], Chihiro Kataoka[2], Daigo Yokoyama[2], Naotoshi Fujita[3], Naruomi Yasuda[4], Akihiro Sugiura[4] and Yoshie Kodera[2]

[1]*Graduate School of Medical Sciences, Nagoya University, Nagoya 461-8673, Japan*
[2]*School of Health Sciences, Nagoya University, Nagoya 461-8673, Japan*
[3]*Department of Radiological Technology, Nagoya University Hospital, Nagoya 466-8560, Japan*
[4]*School of Health Sciences, Gifu University of Medical Science, Seki 501-3892, Japan*
[*]*E-mail address: aihori0312@gmail.com*

(Received November 14, 2010; Accepted April 10, 2011)

In soft-copy diagnosis, each pixel of an X-ray detector is displayed as the corresponding pixel of a liquid crystal display (LCD). However, when a mammographic image is displayed on an LCD for the first time, the entire image is reduced. We examined the influence of differences in LCD image-reduction rates on the signal-detection performance by observational experiments. We created a simulated image similar to Burger's phantom and reduced it by using the nearest neighbor, bilinear, and bicubic interpolation methods. We displayed the reduced images on LCDs with different numbers of pixels and examined the signal-detection performance with each interpolation method. The signal-detection performance deteriorated as the image-reduction rate increased irrespective of the interpolation method. Among the interpolation methods, the nearest neighbor method resulted in the worst signal-detection performance, and the bilinear method was the most suitable for image reduction. Mammographic images are mostly reduced for viewing on an LCD. Such reduction changes the appearance of microcalcifications. Therefore, depending on their size and distribution, microcalcifications observed in these images may be missed on an LCD.

Key words: Liquid Crystal Display, Interpolation Method, Phase-Contrast Mammography, Simulation Image

1. Introduction

Recently, hospitals have begun to digitize medical images. Further, medical-image diagnostic systems are changing from films to liquid crystal displays (LCDs), increasing the need for LCDs as diagnostic monitors. The image quality of LCDs differs according to the purpose and environment. Especially, high image quality is required to display mammographic and chest X-ray images, including those of microscopic lesions and low-contrast shadows. Therefore, higher image quality than that of the conventional X-ray films is necessary for good display performance of LCDs (Pisano *et al.*, 2005).

In soft-copy diagnosis, each pixel of an X-ray detector is displayed as the corresponding pixel of an LCD. Even with high-resolution LCDs, not all pixels of a mammographic image can be displayed on 1 screen, because of the high number of pixels of such images. Especially, magnified images obtained by phase-contrast mammography (PCM) have about 70-million pixels (Thoyama *et al.*, 2006). PCM has an edge emphasis effect on the object and the highest image resolution at 25-μm pixel pitch. Therefore, lesions such as microcalcifications and tumors can be clearly viewed in PCM images compared with the conventional mammographic images. For phase-contrast imaging, the object and the X-ray detector should be located at some distance from each other, then it is magnification radiography. Because PCM images are obtained by a half-cut size cassette, it is impossible to display them on 1 screen even by using an LCD of 5-million pixels, the recommended diagnostic monitor for such images. When a PCM image is displayed on an LCD for the first time, the entire image is reduced. Doctors diagnose breast cancer by using mammograms; therefore, the entire image should be displayed to enable identification of any abnormality, and the diagnostic performance decreases when the entire image is not displayed on the LCD. In addition, images of both breasts are displayed on the LCD simultaneously; therefore, the image-reduction rate of a 2-image LCD increases compared with that of a single-image LCD.

In this study, we created a simulated image of microcalcifications and examined alteration in the shape of their signals in images reduced by using various interpolation methods. We aimed to find a suitable interpolation method for reducing PCM images on LCDs and improving the current LCD-based diagnostic technology.

2. Methods

2.1 Simulated image

A mammographic finding indicating breast cancer is microcalcification, consisting of a small calcium deposit of 0.2–0.5 mm diameter (dos Santos Romualdo *et al.*, 2009). We created a simulated image of microcalcifications similar to Burger's phantom (Fig. 1), which changes the diameter and contrast of round signals. A round signal imitates a microcalcification in a mammographic image.

The simulated image was composed of 288 round signals in 18 rows and 16 columns. In the vertical direction, the diameter of the signals increased logarithmically from 1 to

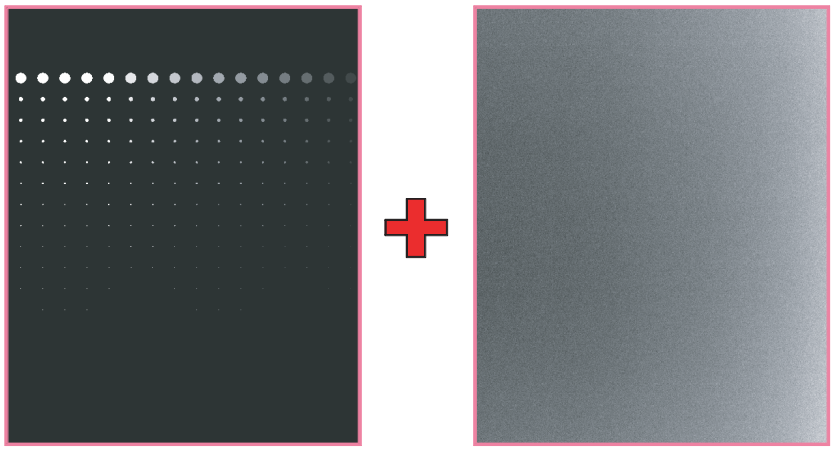

Fig. 1. Simulated image comprising 18 rows and 16 columns. The left signals have higher contrast than the right signals. The signal diameter reduces toward the bottom, and the signals in the lower right region are difficult to detect. The simulated image was merged to an image uniformly exposed by PCM at 24 kV and 25 mAs.

Table 1. Image-reduction rate.

LCDs	Number of Pixels/LCD	Reduction rate (%)	Number of Pixels/Reduced image
2 million	1200 × 1600	16.87	1105 × 1480
3 million	1536 × 2048	21.60	1430 × 1916
5 million	2028 × 2560	27.00	1625 × 2177
5 million (split-screen display)	1023 × 1370	14.46	910 × 1219

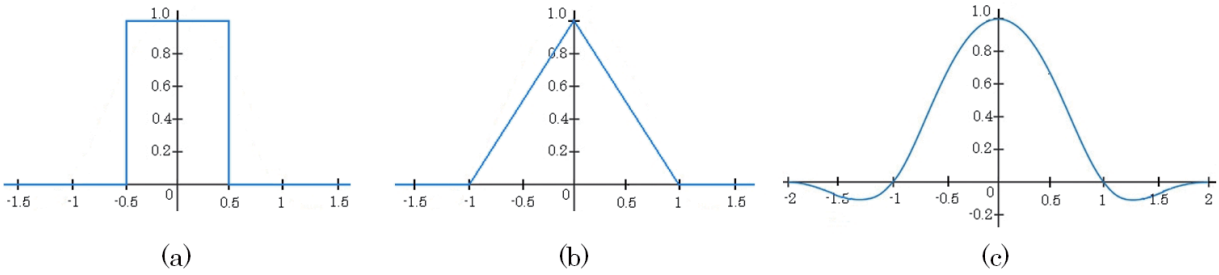

Fig. 2. Interpolation functions (a) nearest neighbor method (b) bilinear method (c) bicubic method.

200 pixels. In the horizontal direction, the pixel value of the signals increased by 5% from 5% to 95% against the background (Ishida *et al.*, 1984). The simulated image was merged to an image uniformly exposed by PCM at 24 kV and 25 mAs. Its matrix size was the same as that of the PCM image.

2.2 Image-reductionrate

The image-reduction rate was calculated as the ratio of the number of pixels per LCD to that per reduced image when the simulated image was displayed on LCDs of 2-, 3-, and 5-million pixels. Moreover, we examined the signal-detection rate at specific image-reduction rates when displaying right and left mammographic images simultaneously on a 5-million-pixel LCD. Table 1 shows the number of pixels per LCD used in this study and the corresponding image-reduction rates.

2.3 Interpolation methods

The simulated image was reduced by using 3 interpolation methods: the nearest neighbor, bilinear, and bicubic methods (Parker *et al.*, 1983; Lehmann *et al.*, 1999). Figure 2 shows the waveform of each function.

2.3.1 Nearest neighbor method From a computational standpoint, the easiest interpolation algorithm to implement is the so-called nearest neighbor algorithm, in which each pixel is given the value of the sample closest to it. Four grid points are needed to evaluate the interpolation function in the 2-dimensional nearest neighbor method. The interpolation kernel for each direction is as follows:

$$ {}^{\text{Nearest}-\text{neighbor}}h(x) = \begin{cases} 1, & 0 \le |x| < 0.5 \\ 0, & \text{elsewhere.} \end{cases} \tag{1} $$

Therefore, strong aliasing and blurring effects are associated with the nearest neighbor method for image interpolation.

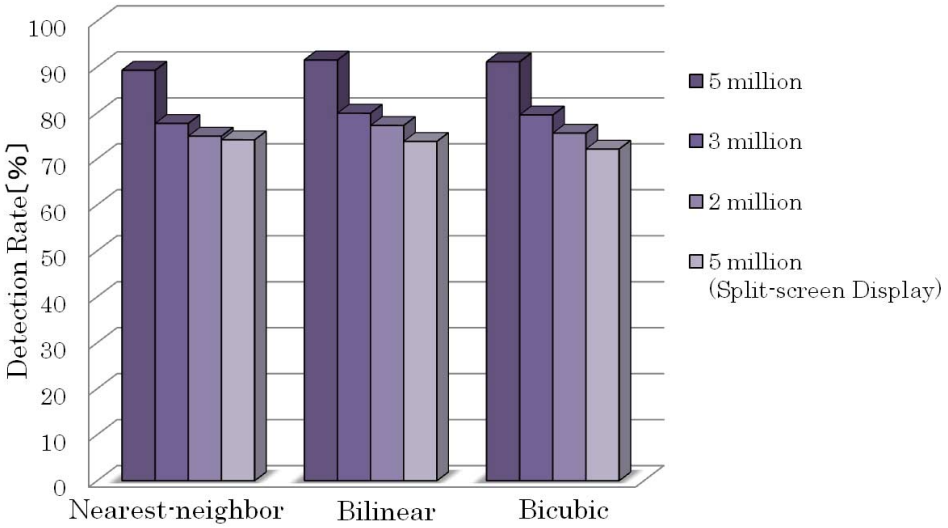

Fig. 3. Results of the observational experiment for comparing the signal-detection performances among the image-reduction rates.

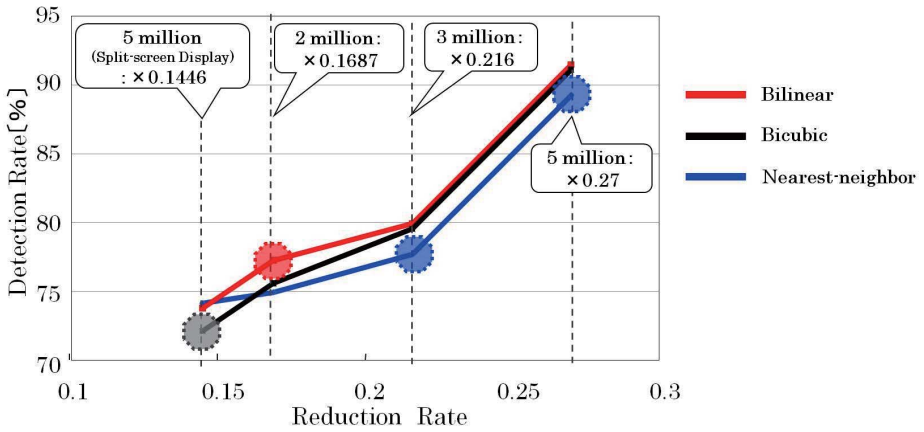

Fig. 4. Results of the observational experiment for comparing the detection performances among the interpolation methods. The circles indicate values significantly different from those obtained with the other methods.

2.3.2 Bilinear method For separated bilinear interpolation, the values of both direct neighbors are weighted by their distance to the opposite point of interpolation. For linear interpolation, the interpolation kernel is as follows:

$$ {}^{\text{Bilinear}}h(x) = \begin{cases} 1 - |x|, & 0 \le |x| < 1 \\ 0, & \text{elsewhere,} \end{cases} \tag{2} $$

where x is the distance between the point to be interpolated and the grid point being considered. The triangular function corresponds to a modest low-pass filter in the frequency domain. Therefore, the main disadvantages of linear interpolation are attenuation of the high-frequency components and aliasing of the data beyond the cutoff point into the low frequencies (Parker *et al.*, 1983).

2.3.3 Bicubic method Cubic convolution interpolation determines the grey level value from the weighted average of the 16 closest pixels to the specified input coordinates and assigns that value to the output coordinates. The kernel is positive in the interval from zero to 1 and negative from 1 to 2. Frequencies directly below the cutoff point are amplified slightly, and the transition between the pass band and the stop band is quite sharp. The cubic convolution interpolation kernel is as follows:

$$ {}^{\text{Bicubic}}h(x) = \begin{cases} (a+2)|x|^3 - (a+3)|x|^2 + 1, & 0 \le |x| < 1 \\ a|x|^3 - 5a|x|^2 + 8a|x| - 4a, & 1 \le |x| < 2 \\ 0, & \text{elsewhere,} \end{cases} \tag{3} $$

where x is the distance between the point to be interpolated and the grid point being considered and a is usually set to -0.5 or -0.75. In this study, we set a to -0.5.

2.4 Observational experiments

For the observational experiments, the room illumination was set to about 50 lx. The window width was a difference between the maximum value and the minimum value of the pixel value obtained from the histogram of the simulation picture. The window level was center values between the maximum value and the minimum value. The window width and level were fixed at 847 and 531, respectively. We set the maximum luminance of the LCD to 500 cd/m^2, and the viewing distance from the LCD was arbitrary. The reduced images were randomly displayed on a 5-million-pixel LCD by using the same software and the signal-detection

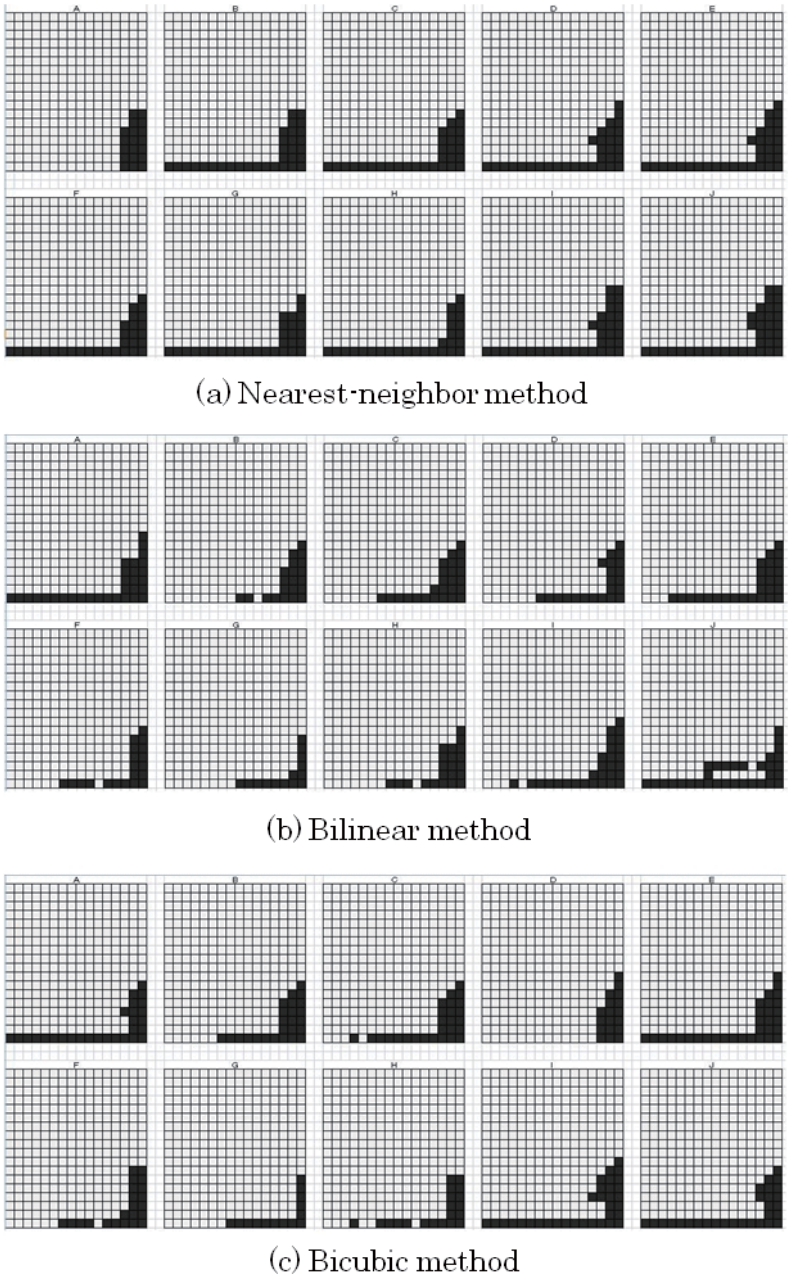

Fig. 5. Answer sheets of the 10 observers when the images were reduced on the 5-million-pixel LCD. The black and white squares indicate undetected and detected signals, respectively. The squares are sequentially arranged from the bottom according to signals of 1-pixel, 2-pixel, 3-pixel, and 4-pixel sizes, representing microcalcifications of 0.05-, 0.06-, 0.08-, and 0.10-mm diameter, respectively.

performance with each interpolation method was examined. Six students who are learning about radiography in the university and four graduate students in a master's course participated as observers. They viewed the reduced images and reported whether the signals could be detected. We defined the signal-detection rate as the ratio of the number of detected signals to the number of all signals. This study was approved by the ethics committee of Nagoya University.

3. Results

Figure 3 shows the results of the observational experiment for comparing the signal-detection performances among the image-reduction rates. The signal-detection performance deteriorated as the image-reduction rate increased irrespective of the interpolation method. There was no significant difference between the 2-million-pixel and the 5-million-pixel split-screen LCDs with the nearest neighbor method ($p < 0.05$ by Scheffe's paired comparison). However, the other groups showed significant differences.

Figure 4 shows the results of the observational experiment for comparing the signal-detection performances among the interpolation methods. When the image-reduction rate was high, the nearest neighbor method resulted in the worst signal-detection performance, whereas the bicubic method caused the worst signal-detection performance at a low image-reduction rate.

Figure 5 shows the answer sheets of the 10 observers when the images were reduced on the 5-million-pixel LCD.

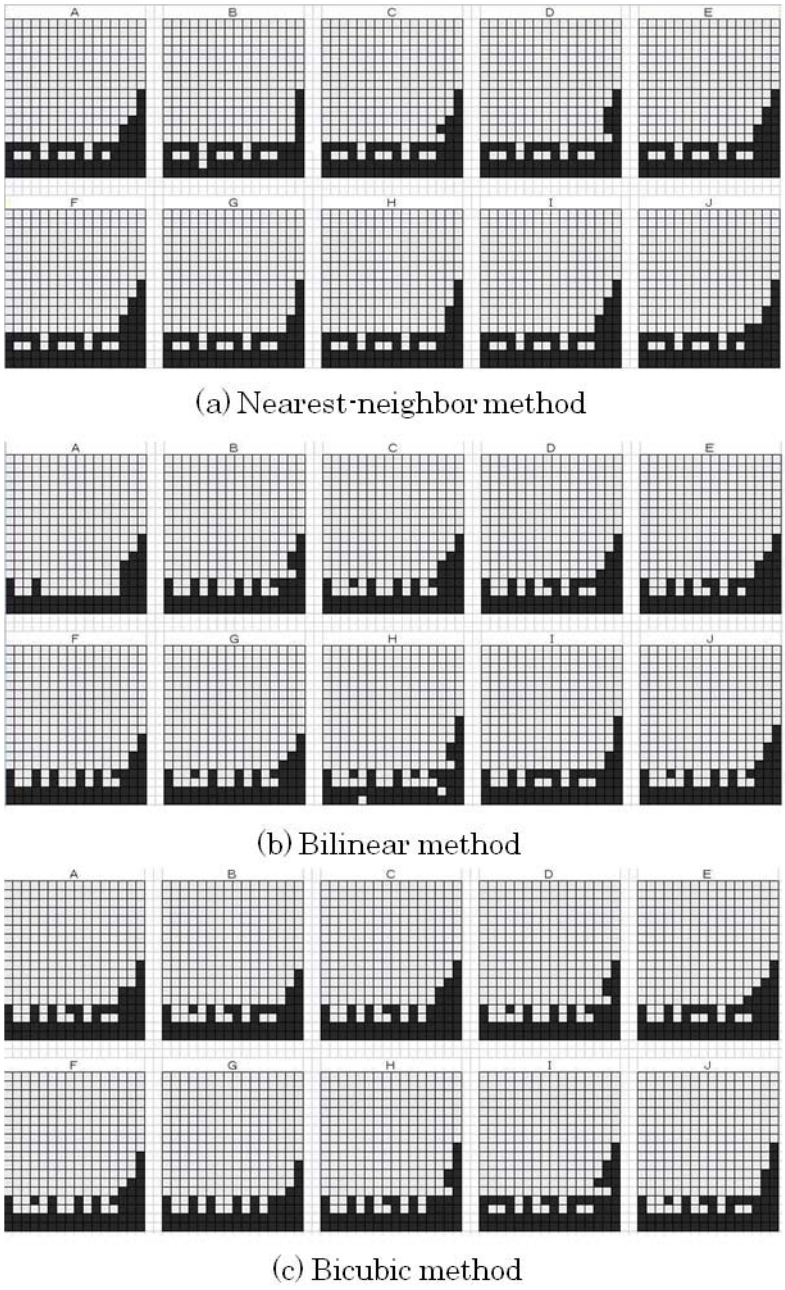

Fig. 6. Answer sheets of the 10 observers when the images were reduced on the 3-million-pixel. The black and white squares indicate undetected and detected signals, respectively. The squares are sequentially arranged from the bottom according to signals of 1-pixel, 2-pixel, 3-pixel, and 4-pixel sizes, representing microcalcifications of 0.05-, 0.06-, 0.08-, and 0.10-mm diameter, respectively.

Because of their small diameter and low contrast, the signals located at the bottom-right of the reduced images were not detected.

Figure 6 shows the answer sheets of the 10 observers when the images were reduced on the 3-million-pixel. The 2 bottom-most lines, representing signals of 1-pixel and 2-pixel sizes and indicating microcalcifications of 0.05- and 0.06-mm diameter, respectively, were not detected with any interpolation method. However, there was a clear demarcation between the signals that could be detected and those that could not be detected from the third and fourth bottom-most lines (microcalcifications of 0.08- and 0.10-mm diameter, respectively).

4. Discussion

The 5-million-pixel LCD is recommended for diagnosing mammographic images because the signal-detection rate at this size is higher than that at the other sizes. However, the signal-detection performance deteriorates as the image-reduction rate increases. When the image-reduction rate is high, signals disappear in the reduction process because of their small size. In general, the size of an image does not change because it is displayed on an LCD suitable for its size. However, in this study, we displayed all the images on a 5-million-pixel LCD. Therefore, the entire image reduced as the image-reduction rate increased and the difference in the image size influenced the signal-detection performance. When the image-reduction rate was high,

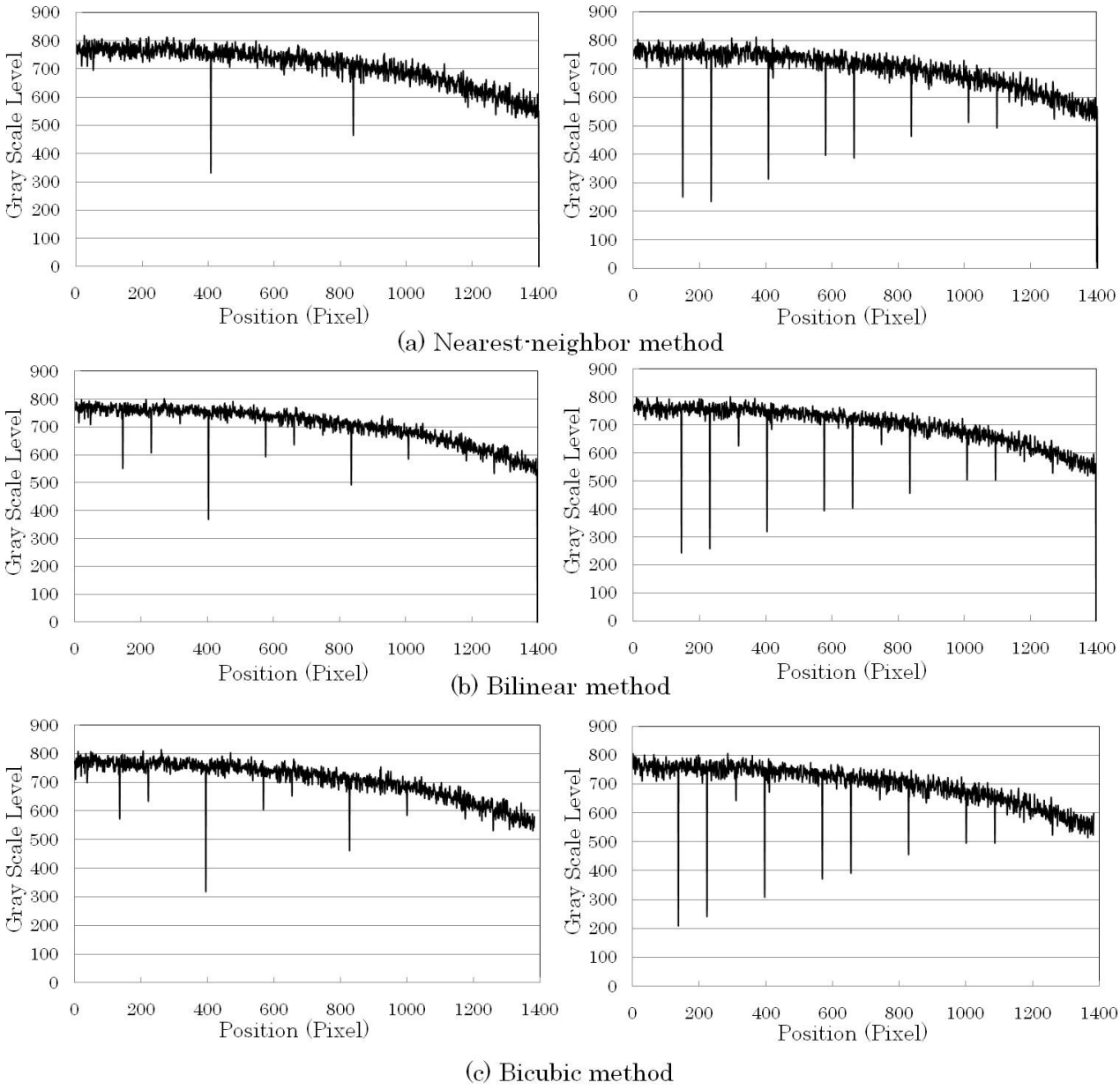

Fig. 7. Profiles of the interpolation methods for the 3-pixel (0.08 mm, right image) and 4-pixel (0.10 mm, left) signals of the 3-million-pixel.

the signal-detection performance with the nearest neighbor method was worse than that with the other interpolation methods. The nearest neighbor method involves substitution of a value closest to the position to be detected. Therefore, the noise property deteriorates and the signal-detection rate decreases in this method. When the image-reduction rate was low, the signal-detection performance with the bicubic method was the worst. Because the function of the bicubic method had a negative value, the noise was emphasized as the image-reduction rate increased. At all the image-reduction rates, the bilinear method yielded the best results.

When the image-reduction rate was high, only small and low-contrast signals were not detected. However, as the rate of image reduction decreased, small signals should not necessarily disappear, and the signals that could not be detected became a periodic form. Figure 7 shows the profiles of the interpolation methods for 3-pixel (microcalcification of 0.08-mm diameter) and 4-pixel (microcalcification of 0.10-mm diameter) signals of the 3-million-pixel LCD. These profiles indicate that the signals disappeared periodically when the image was reduced and they exhibited different cycle regularities when the signals disappeared depending on the interpolation method. The signal-detection rate was lower with the nearest neighbor method than with the other interpolation methods. The result is noteworthy because not only small signals but also several 0.1-mm-diameter signals disappeared in this method.

5. Conclusions

The signal-detection performance deteriorates as display size in the LCD became small. The bilinear method is the most suitable for image reduction.

Mammographic images are mostly reduced for viewing

on LCDs. Such reduction changes the appearance of microcalcifications. Therefore, depending on their size and distribution, such lesions may be missed on LCDs. In addition, microcalcifications of 0.1-mm diameter might disappear when a mammographic image is reduced by using the nearest neighbor method; such images should be displayed on LCDs with fewer pixels.

References

dos Santos Romualdo, L. C., da Costa Vieira, M. A. and Schiabel, H. (2009) Mammography Images Restoration by Quantum Noise Reduction and Inverse MTF Filtering, SIBGRAPI, 180–185, 2009 XXII Brazilian Symposium on Computer Graphics and Image Processing.

Ishida, M., Doi, K., Loo, L. N. *et al.* (1984) Digital image processing: Effect on detectability of simulated low-contrast radiographic patterns, *Radiology*, **150**, 569–575.

Lehmann, T. M., Gonner, C. and Spitzer, K. (1999) Interpolation methods in medical image processing, *IEEE Trans. Med. Imag.*, **18**(11), 1049–1075.

Parker, A. J., Kenyon, R. V. and Troxel, D. E. (1983) Comparison of interpolating methods for image resampling, *IEEE Trans. Med. Imag.*, **2**(1), 31–39.

Pisano, E. D., Gatsonis, C., Hendrick, E. *et al.* (2005) Diagnostic performance of digital versus film mammography for breast cancer screening, *N. Engl. J. Med.*, **353**, 1773–1783.

Thoyama, K., Katafuchi, T. and Matsuo, S. (2006) Clinical implications of phase-contrast imaging in mammography, *Medical Imaging and Information Sciences*, **23**(2), 79–84.